

Structural transformations of double-walled carbon nanotube bundle under hydrostatic pressure

Xiaoping Yang,^{*}) Gang Wu,^{†)} and Jinming Dong^{‡)}

*National Laboratory of Solid State Microstructures and Department of Physics,
Nanjing University, Nanjing 210093, P. R. China*

(Dated: February 1, 2008)

Abstract

Three kinds of the response mechanisms to the external pressure have been found for double-walled carbon nanotube (DWNT) bundle, depending strongly on their average radius and symmetry. The small-diameter DWNT bundle undergoes a small discontinuous volume change, and then deform continuously. The intermediate-diameter DWNT bundle collapses completely after a structure phase transition (SPT). Significantly, two SPTs exist for the larger-diameter DWNT bundle if the outer tube has no C_6 or C_3 symmetry. It would be interesting to search for signatures of these different structural transformations by experimentally investigating mechanical, optical and thermal response functions of DWNT bundle.

PACS numbers: 61.50.Ks, 62.50.+p, 81.07.De, 61.46.-w

It is well known that the physical properties of the carbon nanotubes (CNTs) depend much on their geometrical structures, and so can be easily changed by an applied pressure or strain, which could be used to fabricate the nanoscale electromechanical coupling devices and transducers. For example, a uniaxial strain on the single-walled carbon nanotubes (SWNTs) can cause a metal-semiconductor transition¹.

Recently, the effect of hydrostatic pressure on the CNT bundle has attracted much attention in experiments^{2,3,4,5,6,7,8,9,10}, including the Raman spectroscopy, and theoretical calculations^{11,12,13,14}. The study of the SWNT bundles indicates the Raman peaks shift to higher frequencies with increasing hydrostatic pressure, and the radial breathing mode (RBM) disappears from the spectrum above the critical pressure, showing a SPT. On the other hand, there are much fewer studies of the hydrostatic pressure's effect on the DWNT bundle, which is the simplest multi-walled carbon nanotubes (MWNTs). Very recently, the Raman measurements on the DWNT materials under hydrostatic pressure^{2,3,4} have found the RBM intensity of the outer tubes decreases rapidly with increasing pressure, exhibiting a similar behavior to that of SWNT^{5,6,7,8,9,10,11,12,13}, but the inner tubes appear to be considerably less sensitive to the pressure, e.g., the pressure coefficient of the inner tube is 45% smaller than that of the outer tube.

Therefore, in this work, we intend to study the structural change of DWNT bundles under hydrostatic pressure. Our numerical results show that the symmetry and diameter of outer tube decide mainly the change of cross section and response behavior of DWNT bundles under the pressure. More importantly, two SPTs are found to exist in some DWNT bundles if their outer tubes have the larger diameters and no C_6 or C_3 symmetry.

The zero-temperature structural minimizations of the enthalpy ($H = U + PV$) were carried out on a supercell containing a $2 \times 2 \times 2$ DWNT bundle using the universal force field (UFF) method^{15,16}. In order to induce the SPT, a step-wise increasing hydrostatic pressure was applied to the DWNT bundle, minimizing the enthalpy of the DWNT bundle after each pressure increment.

For (5,5)@(10,10), (7,7)@(12,12) and (9,0)@(18,0) DWNT bundles, we also perform the first principles structure relaxations using the total energy plane-wave potential method¹⁷ in the framework of local density approximation (LDA). The ion-electron interaction was modeled by the projector augmented wave (PAW) method¹⁸ with a uniform energy cutoff of 500 eV. The smearing width was taken to be 0.04 eV in the ground state. And a very good agreement is obtained between the force field and the first principles calculation results (see Table I), indicating that the UFF method is suitable for the system researched in this paper.

The transition pressures, P_c and P_d , for different DWNT bundles are listed in Table II. As we shall see, there exist three kinds of the response behaviors to external pressure, and their loading curves vs hydrostatic pressure are given in Fig. 1(a)-1(c), respectively.

Firstly, for small-diameter (5,5)@(10,10) DWNT bundle, a small discontinuous volume change appears at $P = 18.01$ GPa, accompanied by a cross section's change between two deformed hexagons, as seen from Fig. 1(a). At the same time, the inter tube (5,5) could not collapse with a minimum distance of 4.35 Å between its two opposite walls, which is larger than the distance of 3.4 Å between nearby layers in the turbostratic graphite. If the pressure is increased further, this distance will approach continuously to 3.4 Å. On the other hand, our simulation indicates that the loading curve of (5,5) SWNT bundle [also shown in Fig. 1(a)] varied with external pressure is continuous too and no obvious SPT happens. But (10,10) SWNT bundle collapses at $P_d = 3$ GPa, forming a peanut-shaped cross section with a separation of about 3.4 Å between its two opposite parallel walls. So, it is clear that

existence of an inner (5,5) tube increases the ability of the outer (10,10) tube to resist the applied pressure, making so the (5,5)@(10,10) DWNT bundle do not collapse at 18.01 GPa.

As for the intermediate-diameter DWNT bundles, e.g., the (7,7)@(12,12), (9,9)@(14,14), (10,10)@(15,15), (11,11)@(16,16), (12,12)@(17,17) and (13,13)@(18,18), as shown in Fig. 1(b), it is found that all of them undergo one SPT and collapse completely. Our simulations reveal similar collapses exist for the (7,7), (9,9), (10,10), (11,11), (12,12) and (13,13) SWNT bundles. Taking (10,10)@(15,15) DWNT bundle as an example, its collapse pressure $P_d = 4.68$ GPa that is higher than either that of (10,10) SWNT bundle ($P_d = 3$ GPa) or that of (15,15) SWNT bundle ($P_d = 1.3$ GPa). This means that the outer tube acts as a protection shield, and the inner tube supports the outer one and increase its structure stability. Our results are consistent with the experimental measure results^{2,3,4}.

However, the response behaviors of the larger-diameter DWNT bundles become complex, as shown in Fig. 1(c). The (16,16)@(21,21) and (19,19)@(24,24) DWNT bundles still collapse after one SPT. Surprisingly, the (15,15)@(20,20), (17,17)@(22,22), (18,18)@(23,23) and (21,21)@(26,26) DWNT bundles undergo two different types of SPT with the transition pressure P_c and P_d respectively, accompanied by their cross sections change from deformed hexagon to racetrack first and then to peanut shape, and the DWNT bundles collapse completely after the second SPT. It should be noted that the DWNT bundles exhibit some small discontinuous volume change between the different racetrack-shaped cross sections. We think two SPTs and the racetrack-shaped cross sections could be observed in future experiments if the pressure increment is selected properly.

Furthermore, it is interesting to ask why the racetrack-shaped cross sections do not appear for the (16,16)@(21,21) and (19,19)@(24,24) DWNT bundles before their final collapse? Our simulations reveal that not only their cross sections, but also the ones of the intermediate-diameter DWNT bundles: (7,7)@(12,12), (10,10)@(15,15), (13,13)@(18,18) remain relatively the better hexagon with almost equal sides and corners just before the SPTs, which are different from the other DWNT bundles with the deformed hexagonal or racetrack cross sections before the SPT (in Fig. 1(b)-1(c) we only show the cross sections of some DWNTs, e.g., the (9,9)@(14,14), (10,10)@(15,15), (13,13)@(18,18), (16,16)@(21,21) and (18,18)@(23,23) as examples). It is known that the symmetry group of the isolate (n,n) and (n,0) SWNT is $T_2^1 D_{nh}$. The symmetries of T_2^1 and σ_h are retained under pressure, but in the bundle the cross section symmetry is reduced from D_n to C_6 for the specific outer tubes: (12,12), (18,18) and (24,24), and to C_3 for the (15,15) and (21,21) tubes. A necessary condition to form an ideal hexagonal lattice is that the tube itself has a C_6 rotational axis, and C_3 symmetry can also be somewhat matched to the hexagonal lattice symmetry. Thus, with increasing pressure, these outer tube's cross section can keep better hexagon before the SPT. More importantly these DWNT bundles only undergo one SPT to reach the stable collapsed structure no matter how big is the diameter. On the other hand, the DWNT bundles in which only their inner tubes have the C_6 or C_3 symmetry, for example the (9,9)@(14,14), (12,12)@(17,17), (15,15)@(20,20), (18,18)@(23,23) and (21,21)@(26,26), have still the deformed hexagonal or racetrack-shaped cross sections just before the SPT, and two SPTs would happen with increased diameters. So, the symmetry of the outer tube is a very important factor to decide the cross section shape of the DWNT under the pressure, and comparatively the effect of their inner tube is very small.

We have also studied the structure transformations of zigzag@zigzag DWNT bundles under the hydrostatic pressure, which are found to show a qualitatively same response mechanism to external pressure with the armchair@armchair DWNT bundles, as indicated

by Table II.

Finally, in order to have an insight into the relationship of the collapse pressure P_d with the DWNT diameter and its tube symmetry, we introduce the DWNT's average radius R_{ave} , which is defined as an average value of the outer and inner tube's radius of DWNT. Here we show the variation of P_d with R_{ave} in Fig. 2, from which it can be seen that the collapse pressure can be well fitted to $\sim 1/R_{ave}^3$ for the DWNT bundles. It is known that the tube-tube coupling in a bundle is described by the van der Waals force, which has a small effect on the bundle's collapse pressure. And both the SWNT and DWNT can be described by the continuum elasticity theory as the continuous hollow cylinders. So their bundles would have similar response to the hydrostatic pressure, and the only difference is that the effective radius of DWNT is the average of inner and outer tubes' radius. On the other hand, it has been proved by the continuum elasticity theory [19] and the molecular dynamics simulations [20] that the P_d of an individual SWNT is inversely proportional to its cubic radius. Thus, it is reasonable that the relation of $P_d \sim 1/R_{ave}^3$ appears in the DWNT bundle. In addition, for the DWNT bundles in which the outer tube has C_6 or C_3 symmetry, the collapse pressure is larger than the fitted result. This phenomenon is more obvious, especially for the zigzag@zigzag DWNT bundles, e.g., the (9,0)@(18,0), (15,0)@(24,0), (21,0)@(30,0), (27,0)@(36,0) and (33,0)@(42,0). The reason is that both of their outer and inner tubes have C_6 or C_3 symmetry, further enhancing the matching to the hexagonal lattice and increasing the structure stability of the system. This means the matching between the DWNT symmetry and the lattice symmetry can increase the ability of the DWNT bundle to resist the applied pressure.

In addition, we have also made simulation on the (11,2)@(12,12) DWNT bundle, which is composed of two coaxial SWNTs with different chiral angles, and the result is shown in Table I, Fig. 1(b) and 2. The period of tube (11,2) is just seven times larger than that of tube (7,7), and its radius is equal to that of (7,7). It can be found from Fig. 1(b) that the (7,7)@(12,12) and (11,2)@(12,12) DWNT bundles have the slightly different collapsed pressures of $P_d = 10.6$ GPa and 11.51 GPa, respectively, i.e. the chiral symmetry of the inner tubes in the DWNT bundle has a smaller effect on their collapse pressures.

In summary, our calculations show that the structural transformations of DWNT bundles under hydrostatic pressure is different from those of the SWNT bundles^{5,6,7,8,9,10,11,12,13} and isolate DWNT²¹. One or two SPTs exist depending on the symmetry and diameter of DWNT bundles, which manifest the complexity of nanotubes. It would be interesting to experimentally determine mechanical (e.g., compressibility), optical (e.g., Raman spectrum) and thermal (e.g., heat capacity) response functions of DWNT bundles to search for signatures of these different types of structural transformations.

Acknowledgments

This work was supported by the Natural Science Foundation of China under Grant Nos. 10474035, 90503012, and 10304007, and also by the State Key program of China through Grant No. 2004CB619004.

-
- * Also at: Department of Physics, Huainan Normal University, Huainan, Anhui 232001, P. R. China; Electronic address: bunnyxp@hotmail.com
- † Present address: Department of Physics, National University of Singapore, Singapore 117542
- ‡ Corresponding author. Email address: jdong@nju.edu.cn
- ¹ Liu Yang and Jie Han, Phys. Rev. Lett. **85**, 154 (2000).
 - ² P. Puech, H. Hubel, D.J. Dunstan, R.R. Bacsa, C. Laurent, and W.S. Bacsa, Phys. Rev. Lett. **93**, 095506 (2004).
 - ³ J. Arvanitidis, D. Christofilos, K. Papagelis, K.S. Andrikopoulos, T. Takenobu, Y. Iwasa, H. Kataura, S. Ves, and G.A. Kourouklis, Phys. Rev. B **71**, 125404 (2005).
 - ⁴ J. Arvanitidis, D. Christofilos, K. Papagelis, T. Takenobu, Y. Iwasa, H. Kataura, S. Ves, and G.A. Kourouklis, Phys. Rev. B **72**, 193411 (2005).
 - ⁵ U.D. Venkateswaran, A.M. Rao, E. Richter, M. Menon, A. Rinzier, R.E. Smalley, and P.C. Eklund, Phys. Rev. B **59**, 10928 (1999).
 - ⁶ M.J. Peters, L.E. McNeil, J.P. Lu, and D. Kahn, Phys. Rev. B **61**, 5939 (2000).
 - ⁷ C. Thomsen, S. Reich, A.R. Goni, H. Jantoljak, P.M. Rafailov, I. Loa, K. Syassen, C. Journet, P. Bernier, Phys. Status Solidi B **215**, 435 (1999).
 - ⁸ C. Thomsen, S. Reich, H. Jantoljak, I. Loa, K. Syassen, M. Burghard, G.S. Duesberg, and S. Roth, Appl. Phys. A **69**, 309 (1999).
 - ⁹ J. Tang, L.-C. Qin, T. Sasaki, M. Yudasaka, A. Matsushita, and S. Iijima, Phys. Rev. Lett. **85**, 1887 (2000).
 - ¹⁰ S. Kazaoui, N. Minami, H. Yamawaki, K. Aoki, H. Kataura, and Y. Achiba, Phys. Rev. B **62**, 1643 (2000).
 - ¹¹ M.H.F. Sluiter, V. Kumar, and Y. Kawazoe, Phys. Rev. B **65**, 161402 (2002); M.H.F. Sluiter, and Y. Kawazoe, Phys. Rev. B **69**, 224111 (2004).
 - ¹² J.A. Elliott, J.K.W. Sandler, A.H. Windle, R.J. Young, and M.S.P. Shaffer, Phys. Rev. Lett. **92**, 095501 (2004).
 - ¹³ X.H. Zhang, Z.F. Liu, and X.G. Gong, Phys. Rev. Lett. **93**, 149601 (2004); Siu-Pang Chan, Wai-Leung Yim, X.G. Gong, and Zhi-Feng Liu, Phys. Rev. B **68**, 075404 (2003); X.H. Zhang, D.Y. Sun, Z.F. Liu, and X.G. Gong, Phys. Rev. B **70**, 035422 (2004).
 - ¹⁴ V. Gadagkar, P.K. Maiti, Y. Lansac, A. Jagota and A.K. Sood, Phys. Rev. B **73**, 085402 (2006).
 - ¹⁵ A.K. Rappe, C.J. Casewit, K.S. Colwell, W.A. Goddard, W.M. Skiff, J. Am. Chem. Soc. **114**, 10024 (1992).
 - ¹⁶ N. Yao, V. Lordi, J. Appl. Phys. **84**, 1939 (1998).
 - ¹⁷ G. Kresse, J. Furhmueller, Software VASP, Vienna (1999); G. Kresse, J. Hafner, Phys. Rev. B **47**, R558 (1993); G. Kresse and J. Hafner, Phys. Rev. B **49**, 14251 (1994); G. Kresse, J. Furhmueller, Phys. Rev. B **54**, 11169 (1996); G. Kresse and J. Furthmuller, Comput. Mater. Sci. **6**, 15 (1996).
 - ¹⁸ P.E. Blöchl, Phys. Rev. B **50**, 17953 (1994); G. Kresse and D. Joubert, Phys. Rev. B **59**, 1758 (1999).
 - ¹⁹ B.I. Yakobson, C.J. Brabec, and J. Bernholc, Phys. Rev. Lett. **76**, 2511 (1996).
 - ²⁰ R.B. Capaz, C.D. Spataru, P. Tangney, M.L. Cohen, and S.G. Louie, Phys. Status Solidi B **241**, 3352 (2004); P. Tangney, R.B. Capaz, C.D. Spataru, M.L. Cohen, and S.G. Louie, Nano Letters **5**, 2268 (2005).

²¹ X. Ye, D.Y. Sun, and X.G. Gong, Phys. Rev. B **72**, 035454 (2005).

TABLE

TABLE I: Calculated lattice parameters of some DWNT bundle without external pressure by UFF method and first principles method. a, b and c are the lattice constants of DWNT bundles, and α , β and γ are the angles between the two lattice vectors.

DWNTs bundle	a	b	c	α	β	γ
(5,5)@(10,10)	16.64	16.64	2.44	85.79	94.21	120.16
(5,5)@(10,10) LDA	16.62	16.62	2.45	85.78	94.22	120.09
(7,7)@(12,12)	19.26	19.26	2.44	90.00	90.00	119.98
(7,7)@(12,12) LDA	19.26	19.26	2.45	90.00	90.00	119.98
(9,0)@(18,0)	17.09	17.09	4.23	89.19	91.78	120.01
(9,0)@(18,0) LDA	17.10	17.09	4.24	89.18	91.79	120.01

TABLE II: Calculated critical transition pressure P_c and P_d of DWNT bundles. R_{ave} is the average value of the inner and outer tube's radius in the isolate DWNT directly rolled up from the ideal graphene sheet. The suffix (NC) means at this pressure, no collapse happens.

DWNT bundle	R_{ave}	P_c	P_d
(5,5)@(10,10)	5.085		18.01 (NC)
(7,7)@(12,12)	6.441		10.6
(11,2)@(12,12)	6.441		11.51
(9,9)@(14,14)	7.797		5.1
(10,10)@(15,15)	8.475		4.68
(11,11)@(16,16)	9.153		3.19
(12,12)@(17,17)	9.831		2.39
(13,13)@(18,18)	10.509		2.43
(15,15)@(20,20)	11.865	1.25	1.44
(16,16)@(21,21)	12.543		1.48
(17,17)@(22,22)	13.221	0.97	1.1
(18,18)@(23,23)	13.899	0.7	0.99
(19,19)@(24,24)	14.577		1.02
(21,21)@(26,26)	15.933	0.32	0.7
(7,0)@(16,0)	4.502		30.5 (NC)
(9,0)@(18,0)	5.284		20.24
(11,0)@(20,0)	6.067		12.12
(13,0)@(22,0)	6.85		7.69
(15,0)@(24,0)	7.633		6.61
(17,0)@(26,0)	8.416		4.42
(19,0)@(28,0)	9.199		2.99
(21,0)@(30,0)	9.982		3.61
(23,0)@(32,0)	10.765		1.82
(25,0)@(34,0)	11.548	1.52	1.55
(27,0)@(36,0)	12.331		2.23
(29,0)@(38,0)	13.113	0.85	1.13
(31,0)@(40,0)	13.896	0.71	0.99
(33,0)@(42,0)	14.679		1.01

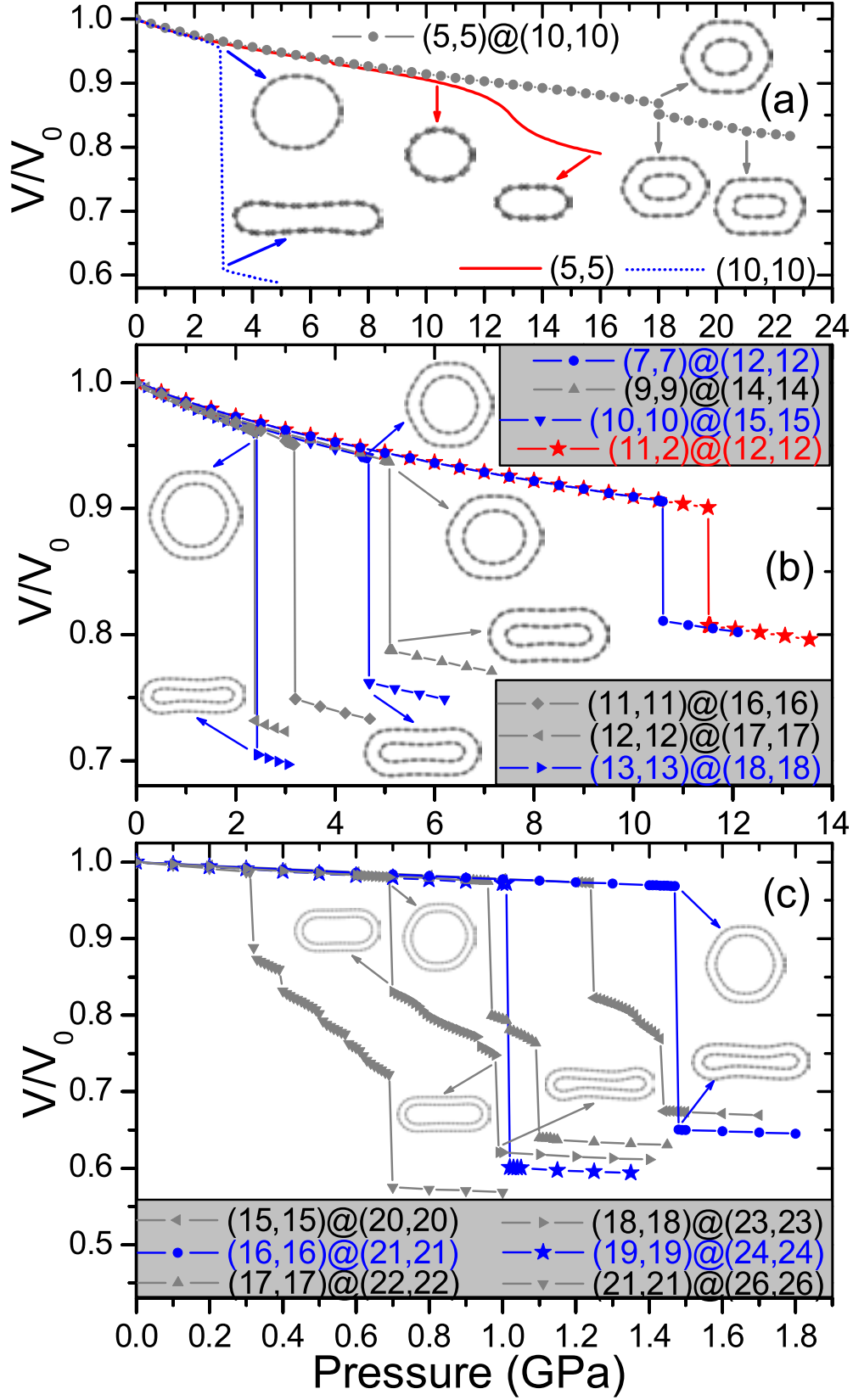


FIG. 1: (Color online) Loading curves for different armchair@armchair DWNT bundles as a function of hydrostatic pressure. (a) small-diameter $(5,5)@(10,10)$ DWNT bundle; (b) some intermediate-diameter DWNT bundles; (c) the larger-diameter DWNT bundles.

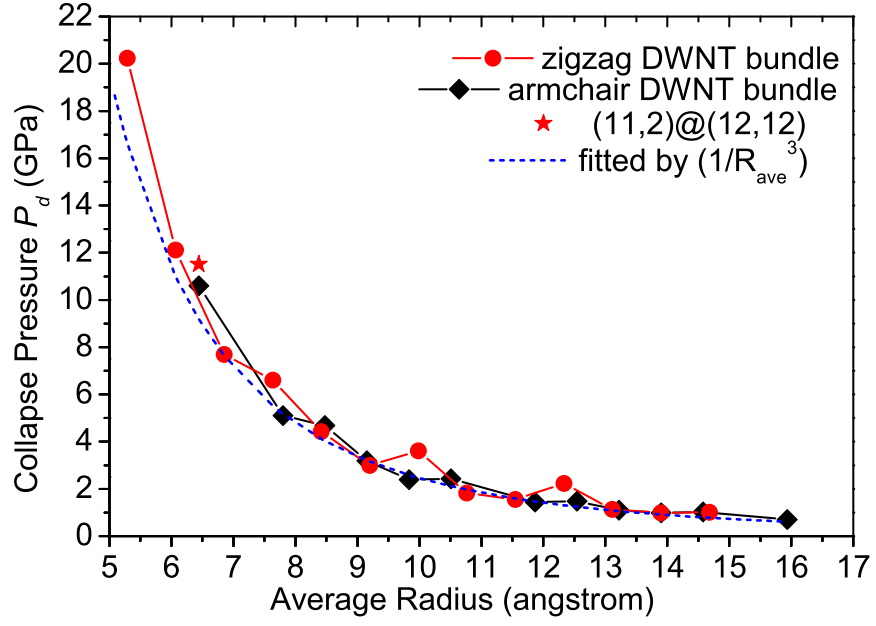


FIG. 2: (Color online) Collapse pressure P_d as a function of the average radius of DWNT. P_d can be well fitted to $\sim 1/R_{ave}^3$.